[Short title + Author Name - P&H title] 17 (2024) 105455

Contents lists available at ScienceDirect

Arabian Journal of Chemistry

journal homepage: www.ksu.edu.sa

Novel quinazolin-4(3*H*)-one bionic-alkaloids bearing an 1,3,4-oxadiazole fragment as potential fungicides inhibiting *Botrytis cinerea*: Design, synthesis and bioactive-guided structural optimization

Xiaobin Wang [a,b,c,*], Lili Yan [a], Juan Zhang [d], Yilin Zhang [a], Zongqun Zhang [a], Quanqing Zhao [a], Qingfang Cheng [a,*], Weihua Zhang [c,*]

[a] *Jiangsu Key Laboratory of Marine Pharmaceutical Compound Screening, College of Pharmacy, Jiangsu Ocean University, Lianyungang 222005, China*
[b] *Jiangsu Institute of Marine Resources Development, Lianyungang 222005, China*
[c] *Jiangsu Key Laboratory of Pesticide Science, College of Sciences, Nanjing Agricultural University, Nanjing 210095, China*
[d] *Research Center of Ocean Engineering Technology, College of Ocean Engineering, Jiangsu Ocean University, Lianyungang 222005, China*

ARTICLE INFO

Keywords:
Quinazolin-4(3*H*)-one
1,3,4-oxadiazole
Discovery of antifungal lead
Botrytis cinerea

ABSTRACT

The ever-rising resistance in *Botrytis cinerea* has appeared as the awkward agricultural challenge that could be effectively resolved by developing novel fungicides featuring disparate action mechanisms. Aiming to explore novel fungicidal leads inhibiting *B. cinerea*, quinazolin-4(3*H*)-one bionic-alkaloids bearing an 1,3,4-oxadiazole fragment were conceived, synthesized, and systematically optimized under the guidance of anti-*B. cinerea* activities. The aforementioned optimization on molecular structures generated the anti-*B. cinerea* candidate $\mathbf{I_{25}}$ owning the promising *in vitro* EC_{50} value (0.76 μg/mL) that was fantastically superior to those of boscalid, penthiopyral, pyrimethanil and imazalil (0.86, 1.03, 15.91 and 2.15 μg/mL). Whereafter, the *in vivo* anti-*B. cinerea* preventative efficacy of an active molecule $\mathbf{I_{25}}$ was noticeably evaluated as 69.3 % at 200 μg/mL, which was megascopically better than that of boscalid (60.6 %). Furthermore, the preliminary investigation on action mechanisms indicated that the fungicidal molecule $\mathbf{I_{25}}$ could induce the conspicuous wrinkle on hyphal surfaces and increase the membrane permeability of *B. cinerea* cells. The above results have emerged as an imperative reference to developing the novel fungicides that could effectively control gray mold caused by *B. cinerea*.

1. Introduction

Botrytis cinerea is a necrotroph fungal pathogen that menacingly infests more than 200 plant species including grape, strawberry, cherry, tomato, cucumber, wheat, rose and lily (Xiong et al., 2019). After suffering an infestation, *B. cinerea* not only generates the particularly functional enzymes that degrade the cell wall of host plants, but also results the phytopathogenic mycotoxins that act on the plant cellular structures including plasma membrane, chloroplast, mitochondria, and so on (Petrasch et al., 2019; Williamson et al., 2007). The above-mentioned changes caused by *B. cinerea* tend to induce the growth retardation, tissue atrophy, leaf necrosis and fruit decay of host plants, which poses a serious threat to the safety production of fruits, vegetables, ornamental flowers and field crops (Dean et al., 2012). Nowadays, the commercialized fungicides including pyrimethanil, azoxystrobin, boscalid remain the most powerful tool to effectively control the gray mold induced by *B. cinerea* (Bardas et al., 2010; Liu et al., 2016). However, the immoderate utilisation of above fungicides has caused the ever-rising resistance in *B. cinerea*, which have been pressing the development of novel fungicide alternatives that own an inimitable

Abbreviations: ^{1}H NMR, ^{1}H nuclear magnetic resonance; ^{13}C NMR, ^{13}C nuclear magnetic resonance; HRMS, High-resolution mass spectrometry; EC_{50}, Median effective concentration; m. p, melting points; $CDCl_3$, deuterochloroform; SEM, scaning electron microscopy; *R. solani*, *Rhizoctonia solani*; *F. graminearum*, *Fusarium graminearum*; *B. cinerea*, *Botrytis cinerea*; *A. solani*, *Alternaria solani*.

Peer review under responsibility of King Saud University. Production and hosting by Elsevier.

* Corresponding authors at: Jiangsu Key Laboratory of Marine Pharmaceutical Compound Screening, College of Pharmacy, Jiangsu Ocean University, Lianyungang 222005, China (Xiaobin Wang).

E-mail addresses: xb_wang@jou.edu.cn (X. Wang), spring817191@sina.com (Q. Cheng), njzhangwh@126.com (W. Zhang).

https://doi.org/10.1016/j.arabjc.2023.105455
Received 17 September 2023; Accepted 11 November 2023
Available online 13 November 2023

action mechanism against *B. cinerea* (Harper et al., 2022; Shao et al., 2021).

Quinazolin-4(3*H*)-one belongs to the nitrogenous heterocyclic fragment that widely exists in the multitudinous secondary metabolites including febrifugine, tryptanthrin, and luotonin A (Fig. 1) as well as the medicinal molecules including methaqualone, diproqualone, albaconazole (Wang et al., 2021). The widespread utilization of above molecules in medicinal chemistries greatly stimulates the search on quinazolin-4(3*H*)-one derivatives that feature various molecular structures and extensive inhibitory effects against phytopathogenic fungi. For instance, fluquinconazole bearing a quinazolin-4(3*H*)-one fragment was arduously developed as the agricultural fungicide that could effectively inhibit the biological synthesis of ergosterol within phytopathogenic fungi (Wang et al., 2019). Recently, some quinazolin-4(3*H*)-one bionic-alkaloids serving as efficient inhibitors against agricultural fungi were successively obtained by optimizing the molecular structures of febrifugine, tryptanthrin, and luotonin A (Hao et al., 2020; Wang et al., 2018; Yang et al., 2020). Concurrently, diverse quinazolin-4(3*H*)-ones bearing a arylimine, 1,2,4-triazolo[3,4-*b*][1,3,4]thiadiazole, amide or 1,2,4-triazole fragment were also documented for their remarkable inhibition effects against phytopathogenic fungi (Du et al., 2018; Lv et al., 2018; Wang et al., 2013; Zhang et al., 2016). Furthermore, our previous work involving the systematical optimization on a tryptanthrin structure indicated that the substituent category at the *N*-3 position of quinazolin-4(3*H*)-one nucleus could significantly influence the inhibitory effect of constructed bionic-alkaloids against agricultural fungi including *B. cinerea* (Wang et al., 2022).

As an important heterocyclic fragment, 1,3,4-oxadiazole has extensively emerged in multitudinous interesting molecules that exhibit anti-inflammatory, antineoplastic, antibacterial, antifungal, antidepressant, antiviral, antiseizure and antioxidant activities (Almalki et al., 2022; Ma et al., 2013; Peng et al., 2021; Rapolu et al., 2013; Rasool et al., 2023; Tantray, 2018; Wang et al., 2023; Zhu et al., 2022). During the last decades, the broad-spectrum activities endowed by 1,3,4-oxadiazole nuclei have inspired their applied research on the development of agricultural chemicals, which resoundingly developed the representative agrochemicals (Fig. 1) including metoxadiazone (insecticide), fubianezuofeng (bactericide), exianliumi (nematicide) and flusulfinam (herbicide) (Gao et al., 2017; Tao et al., 2019; Wang et al., 2020). Recently, some efficient inhibitors against phytopathogenic fungi were tactfully constructed by integrating an 1,3,4-oxadiazole fragment into the molecular structures of natural products including stilbene, mandelic acid, β-carboline and Psoralen (Dong et al., 2022; Jian et al., 2015; Hou et al., 2023; Zhang et al., 2018). Meanwhile, some hydrazide, carboxamide, pyrazole, pyridazinone, azetidin-2-one and sulfone derivatives bearing an 1,3,4-oxadiazole fragment were also documented for their effective inhibitory effects against plant fungi (Chen et al., 2000; Khanum et al., 2009; Long et al., 2021; Xu et al., 2011; Yang et al., 2021; Zou et al., 2002). Obviously, the above-mentioned explorations argue persuasively the potential feasibility for developing novel 1,3,4-oxadiazole agrochemicals that could efficiently inhibit phytopathogenic fungi.

Considering the favourable impact endowed by 1,3,4-oxadiazole fragments on anti-phytopathogenic fungi, the main purposes of this present work mainly are to: (*i*) construct a series of newfangled bionic-alkaloids by rationally integrating an 1,3,4-oxadiazole fragment into the *N*-3 position of quinazolin-4(3*H*)-one nucleus through an alkane bridge, as shown in Fig. 1; (*ii*) estimate the *in vitro* and *in vivo* inhibitory effects of the mentioned-above bionic-alkaloids against phytopathogenic fungi, particularly *B. cinerea*; (*iii*) systematically explore the relevant structure–activity relationship via the structural optimizations guided by fungicidal activities; and (*iv*) investigate the impact of the oxadiazole-containing quinazolin-4(3*H*)-one bionic-alkaloids on mycelium growths by the morphological observation on a scaning electron microscopy (SEM) and the determination against cell membrane permeabilities.

2. Materials and methods

2.1. Instruments and chemicals

The reaction reagents labeled as Adamas brand were purchased from Shanghai Titan Technology Co. Ltd. and were used directly in our present work. The silica gel GF_{254} monitoring reactions and the column chromatography silica gel isolating compounds were both purchased from Shanghai Titan Technology Co. Ltd. The melting points (m. p.) of oxadiazole-containing quinazolin-4(3*H*)-ones were determined *via* an uncorrected SMP50 Digital Melting Point Apparatus (Staffordshire, United Kingdom). The deuterochloroform ($CDCl_3$) containing a target molecule was measured by a Bruker AVANCE III 400 MHz spectrometer (Bruker Corporation, Germany) to generate the corresponding nuclear magnetic resonance spectra (^{1}H NMR and ^{13}C NMR). The methanol containing a target molecule was handled by a Triple TOF 5600 plus LC/MS/MS spectrometer (AB SCIEX, USA) to generate the corresponding

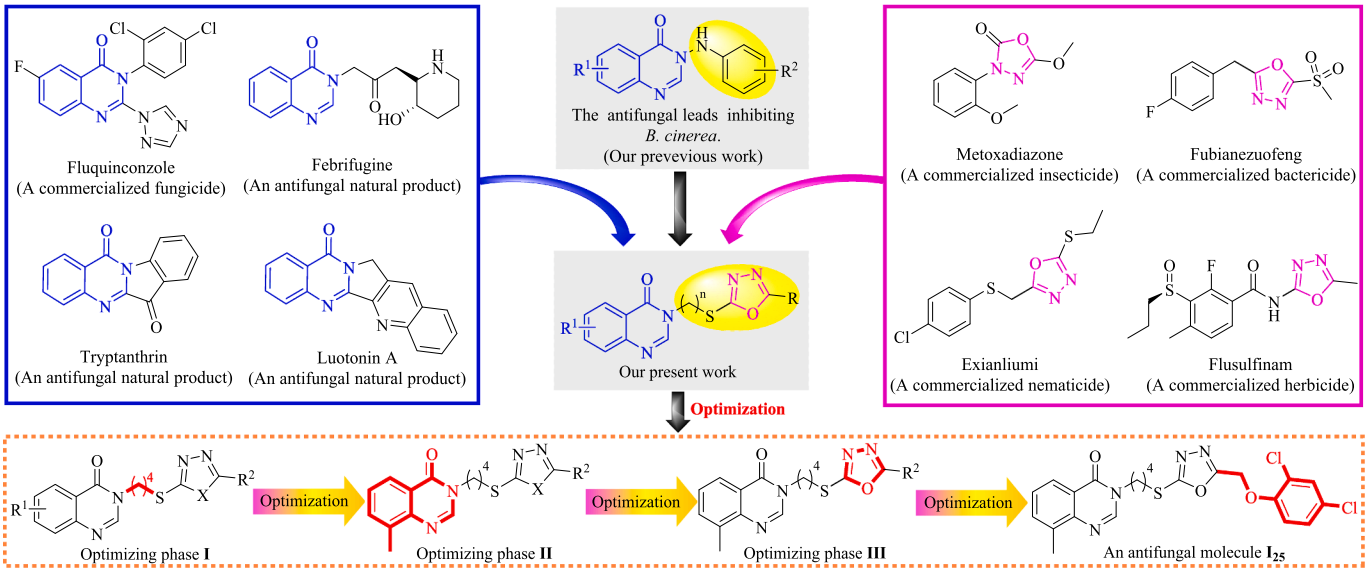

Fig. 1. Design strategy of quinazolin-4(3*H*)-one bionic-alkaloids bearing an 1,3,4-oxadiazole fragment.

High resolution mass spectrometry data (HRMS). The investigation related to mycelial morphologies was carried out on a SU8010 electron microscope (Hitachi, Japan) for generating the corresponding SEM images.

2.2. Synthesis for target compounds I_1–I_{31}

2.2.1. General procedures for synthesizing target compounds I_1–I_6

The important intermediate **3a** named 5-((4-chlorophenoxy) methyl)-1,3,4-oxadiazole-2-thiol and the intermediate **4a** named 8-methylquinazolin-4(3*H*)-one were expediently synthesized via our previous described procedures (Wang et al., 2019). The 8-methylquinazolin-4(3*H*)-one (18.73 mmol) dissolving in 1,4-dioxane (50 mL) reacted with formaldehyde (37 %, 56.19 mmol) under 78 °C for 5 h. After transferring to distilled water (500 mL), the obtained solution visibly generated the white solid that was filtrated to harvest the 3-(hydroxymethyl)-8-methylquinazolin-4(3*H*)-one labelled as an intermediate **5**. After the 3-(hydroxymethyl)-8-methylquinazolin-4(3*H*)-one dissolving in 1,4-dioxane (50 mL) reacted with thionyl chloride (47.32 mmol) under 78 °C for 5 h, the obtained mixture was alkalized by concentrated sodium hydroxide solution until their pH value reached 14, and was subsequently extracted by ethyl acetate (50 mL × 3). The obtained ethyl acetate was dried with anhydrous sodium sulfate, and was removed on a rotary evaporator to prepare the 3-(chloromethyl)-8-methylquinazolin-4(3*H*)-one labelled as an intermediate **6**.

The *N*,*N*-dimethyl formamide (DMF, 40 mL) containing 8-methylquinazolin-4(3*H*)-one (18.73 mmol) slowly mixed with sodium hydride (NaH, 33.71 mmol) in an ice-bath within 30 min. Then, the dibromo alkane (56.19 mmol) dissolving in DMF (10 mL) was slowly added into the above DMF solution in an ice-bath. After stirring for 5 h under 78 °C, the obtained mixture was transferred to distilled water (300 mL), and immediately generated the abundant white solids that were filtrated and then dissolved in dichloromethane (40 mL). After filtrating again, the obtained dichloromethane was removed on a rotary evaporator to prepare the brominated intermediates **7a**–**7e** emerging in Fig. 2. An intermediate **6** or **7** (2.40 mmol) reacted with an intermediate **3a** (2.40 mmol) in the boiling acetonitrile (25 mL) containing potassium carbonate (7.19 mmol) for 3 h. After filtration, the mentioned-above reactant was desolvated under vacuum, and recrystallized with ethanol to expediently construct the oxadiazole-containing quinazolin-4(3*H*)-ones I_1–I_6 that were documented in our previous work (Wang et al., 2021).

2.2.2. General procedures for synthesizing target compounds I_7–I_{10}

The target compounds I_1–I_6 emerging in Fig. 3 were effectively constructed by the procedures that successfully prepared a title compound I_4, in which 2-amino-3-methylbenzoic acid was replaced by a 2-aminobenzoic acid (I_7), 2-amino-5-methylbenzoic acid (I_8), 2-amino-5-chlorobenzoic acid (I_9) or 2-amino-4,5-dimethoxybenzoic acid (I_{10}).

2.2.3. General procedures for synthesizing target compounds I_{11} and I_{12}

The ethanol (50 mL) containing 2-(4-chlorophenoxy)acetohydrazide (**2a**, 14.95 mmol) and potassium hydroxide (KOH, 17.94 mmol) was stirred in an ice-bath for 30 min. After slowly mixing with the carbon disulfide (CS_2, 17.94 mmol) dissolving by ethanol (10 mL) in an ice-bath, the obtained mixture was stirred for 5 h under 20 °C, filtrated and washed by ethanol to obtain the potassium 2-(2-(4-chlorophenoxy) acetyl)hydrazine-1-carbodithioate labelled as an intermediate **8** in Fig. 4. The obtained intermediate **8** (9.53 mmol) slowly mixed with concentrated sulfuric acid (50 mL), and then stirred in an ice-bath for 2 h. After transferring to distilled water (200 mL), the white solids emerging in the above mixture were filtrated, dissolved in 10 % sodium hydroxide solution, and acidized by concentrated hydrochloric acid to obtain the 5-((4-chlorophenoxy)methyl)-1,3,4-thiadiazole-2-thiol labelled as an intermediate **9** in Fig. 4.

The intermediate **8** (9.53 mmol) reacted with hydrazine hydrate (80

A. Synthesis of target compounds I_1-I_6.

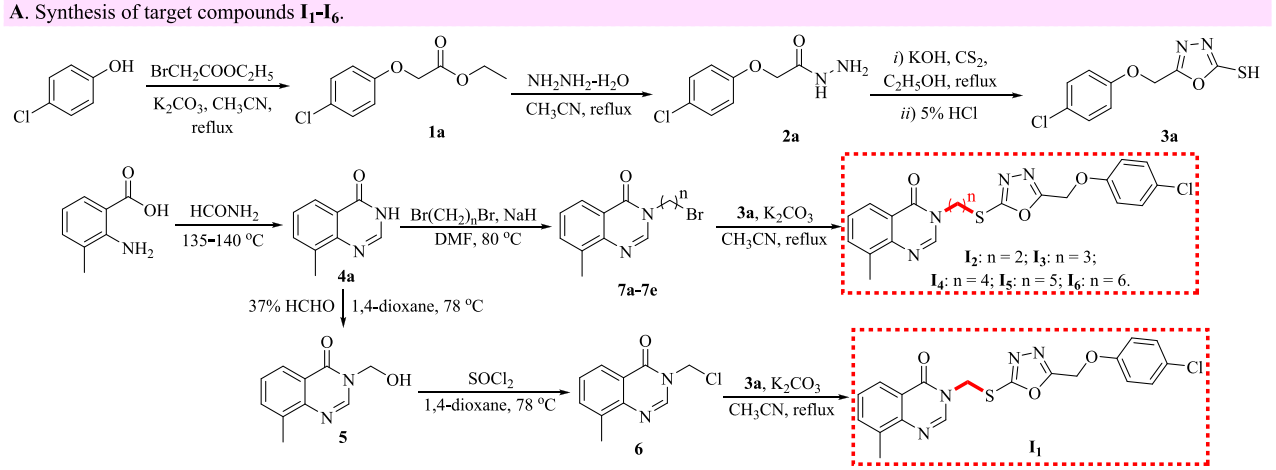

B. Antifungal effects of target compounds I_1-I_6.

Compound	Antifungal effects at 50 μg/mL (%)				EC_{50} values (μg/mL)		
	R. solani	*F. graminearum*	*B. cinerea*	*A. solani*	*R. solani*	*F. graminearum*	*B. cinerea*
I_1	48.13 ± 2.24	20.98 ± 0.90	26.66 ± 1.52	15.74 ± 0.65	> 50	> 50	> 50
I_2	**62.08 ± 2.96**	45.96 ± 0.67	41.43 ±1.14	30.98 ± 0.65	11.20 ± 0.32	> 50	> 50
I_3	**54.24 ± 2.22**	31.48 ± 0.97	46.31 ± 1.22	0.00 ± 0.01	41.90 ± 1.61	> 50	> 50
I_4	**50.37 ± 3.02**	18.21 ± 0.41	**83.32 ± 3.96**	0.00 ± 0.03	53.68 ± 2.44	> 50	**0.92 ± 0.04**
I_5	44.40 ± 1.27	14.26 ± 0.41	39.75 ± 1.73	0.00 ± 0.01	> 50	> 50	> 50
I_6	30.73 ± 0.56	7.94 ± 0.13	30.99 ± 0.49	0.05 ± 0.01	> 50	> 50	> 50

Fig. 2. Synthesis and antifungal effects of target compounds I_1–I_6.

A. Synthesis of target compounds $\mathbf{I_7}$-$\mathbf{I_{10}}$.

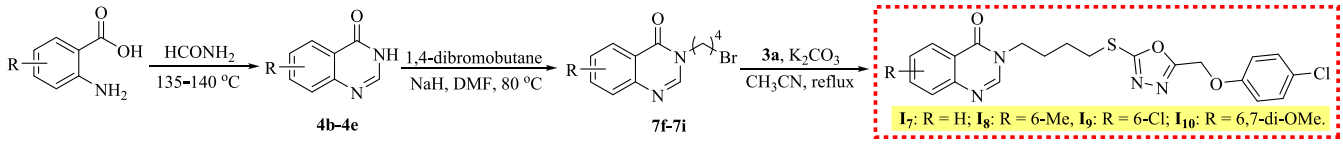

B. Antifungal effects of target compounds $\mathbf{I_7}$-$\mathbf{I_{10}}$.

Compound	Antifungal effects at 50 μg/mL (%)				EC_{50} values against *B. cinerea*		
	R. solani	*F. graminearum*	*B. cinerea*	*A. solani*	Regression equation	*r*	EC_{50} (μg/mL)
$\mathbf{I_4}$	50.37 ± 3.02	18.21 ± 0.41	**83.32 ± 3.96**	15.74 ± 0.65	y = 0.59x + 5.02	0.96	**0.92 ± 0.04**
$\mathbf{I_7}$	44.65 ± 2.05	13.97 ± 0.75	**86.84 ± 1.59**	21.04 ± 1.23	y = 0.92x + 4.63	0.97	**2.53 ± 0.40**
$\mathbf{I_8}$	**60.37 ± 1.37**	38.65 ± 1.50	**61.41 ± 3.35**	9.08 ± 0.56	y = 0.58x + 4.26	0.98	**19.52 ± 1.29**
$\mathbf{I_9}$	**63.78 ± 0.68**	35.16 ± 2.00	**57.18 ± 2.98**	35.91 ± 2.16	y = 0.72x + 4.04	0.96	**21.76 ± 1.34**
$\mathbf{I_{10}}$	**61.51 ± 2.51**	15.71 ± 1.71	43.36 ± 1.15	12.07 ± 1.11	y = 1.23x + 2.86	0.93	54.98 ± 3.07

Fig. 3. Synthesis and antifungal effects of target compounds $\mathbf{I_7}$–$\mathbf{I_{10}}$.

A. Synthesis of target compounds $\mathbf{I_{11}}$ and $\mathbf{I_{12}}$.

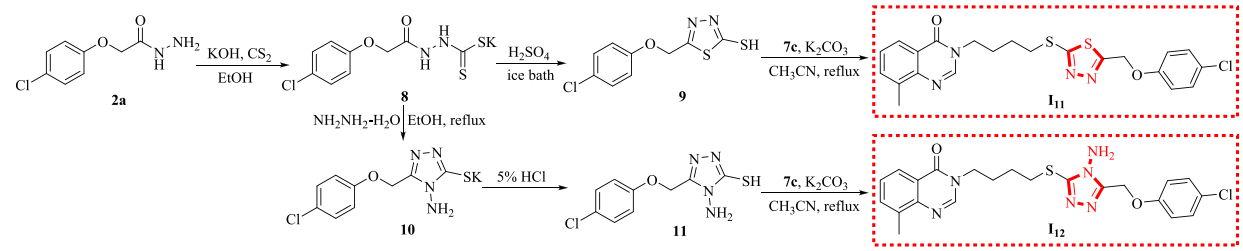

B. Antifungal effects of target compounds $\mathbf{I_{11}}$ and $\mathbf{I_{12}}$.

Compound	Antifungal effects at 50 μg/mL (%)				EC_{50} values against *B. cinerea*		
	R. solani	*F. graminearum*	*B. cinerea*	*A. solani*	Regression equation	*r*	EC_{50} (μg/mL)
$\mathbf{I_4}$	50.37 ± 3.02	18.21 ± 0.41	**83.32 ± 3.96**	15.74 ± 0.65	y = 0.59x + 5.02	0.96	**0.92 ± 0.04**
$\mathbf{I_{11}}$	39.16 ± 1.90	3.16 ± 0.06	**79.01 ± 2.42**	6.24 ± 0.10	y = 0.88x + 4.36	0.97	**5.31 ± 0.52**
$\mathbf{I_{12}}$	19.02 ± 0.35	30.43 ± 0.79	44.73 ± 1.22	4.65 ± 0.08	y = 1.31x + 2.58	0.97	69.94 ± 2.10

Fig. 4. Synthesis and antifungal effects of target compounds $\mathbf{I_{11}}$ and $\mathbf{I_{12}}$.

%, 95.30 mmol) in refluxed ethanol (50 mL) for 5 h. After removing ethanol under vacuum and transferring to distilled water (200 mL), the obtained mixture was acidized by the 5 % hydrochloric acid, and filtered to acquire the 4-amino-5-((4-chlorophenoxy)methyl)-4*H*-1,2,4-triazole-3-thiol labelled as an intermediate **11** in Fig. 4. The intermediate **9** or **11** (2.40 mmol) reacted respectively with an intermediate **7c** (2.40 mmol) in the boiling acetonitrile (25 mL) containing potassium carbonate (7.19 mmol) for 3 h. After filtration, the mentioned-above reactant was desolvated under vacuum, and recrystallized with ethanol to expediently construct the target molecules $\mathbf{I_{11}}$ and $\mathbf{I_{12}}$ emerging in Fig. 4.

2.2.4. General procedures for synthesizing target compounds I_{13}–I_{16}

4-Chlorobenzoic acid or 2-(4-chlorophenyl)acetic acid (63.87 mmol) was stirred in the refluxed ethanol (50 mL) containing concentrated sulfuric acid (6.39 mmol) for 5 h. After removing ethanol under vacuum and transferring to distilled water (100 mL), the resulting mixture was extracted by ethyl acetate (50 mL × 3), dried with anhydrous sodium sulfate, and removed superfluous ethyl acetate on a rotary evaporator to prepare the intermediate **1b** or **1c** emerging in Fig. 5. Concurrently, 4-chlorobenzenethiol (20.74 mmol) reacted with ethyl bromoacetate (24.89 mmol) in the refluxed acetonitrile (50 mL) containing potassium carbonate (31.12 mmol) for 5 h. After filtration, the superfluous acetonitrile in an obtained filter liquor was removed to prepare the colorless oleamen containing an intermediate **1d**. Then, the obtained intermediate **1d** (13.00 mmol) reacted with hydrogen peroxide (H_2O_2, 30 %, 39.00 mmol) in the room-temperature ethanol (40 mL) containing ammonium molybdate ($H_8MoN_2O_4$, 0.65 mmol) for 3 h. After filtration, the resulting filter liquor was removed superfluous ethanol, transferred to distilled water (100 mL), extracted by ethyl acetate (50 mL × 3), and followed by the removal of ethyl acetate on a rotary evaporator to generate the intermediate **1e** emerging as white solids.

After the obtained intermediates **1b–1e** (14.95 mmol) mentioned-above reacted with hydrazine hydrate (80 %, 44.85 mmol) in refluxed acetonitrile (50 mL) for 3 h, the superfluous acetonitrile in the obtained mixture was removed under vacuum to generate the white solids labelled as the intermediates **2b–2e** in Fig. 5. After the obtained intermediate **2** (14.95 mmol) reacted potassium hydroxide (KOH, 17.94 mmol) in chilled ethanol (50 mL) for 30 min, the carbon disulfide (CS_2, 17.94 mmol) dissolving in ethanol (10 mL) was successively added into the above mixture, stirred under reflux for 5 h, transferred to distilled water (300 mL), acidized by the 5 % hydrochloric acid, and filtered to obtain the white solids labelled as the intermediates **3b–3e** in Fig. 5. Subsequently, the obtained intermediates **3b–3e** (2.40 mmol) reacted respectively with an intermediate **7c** (2.40 mmol) in the boiling

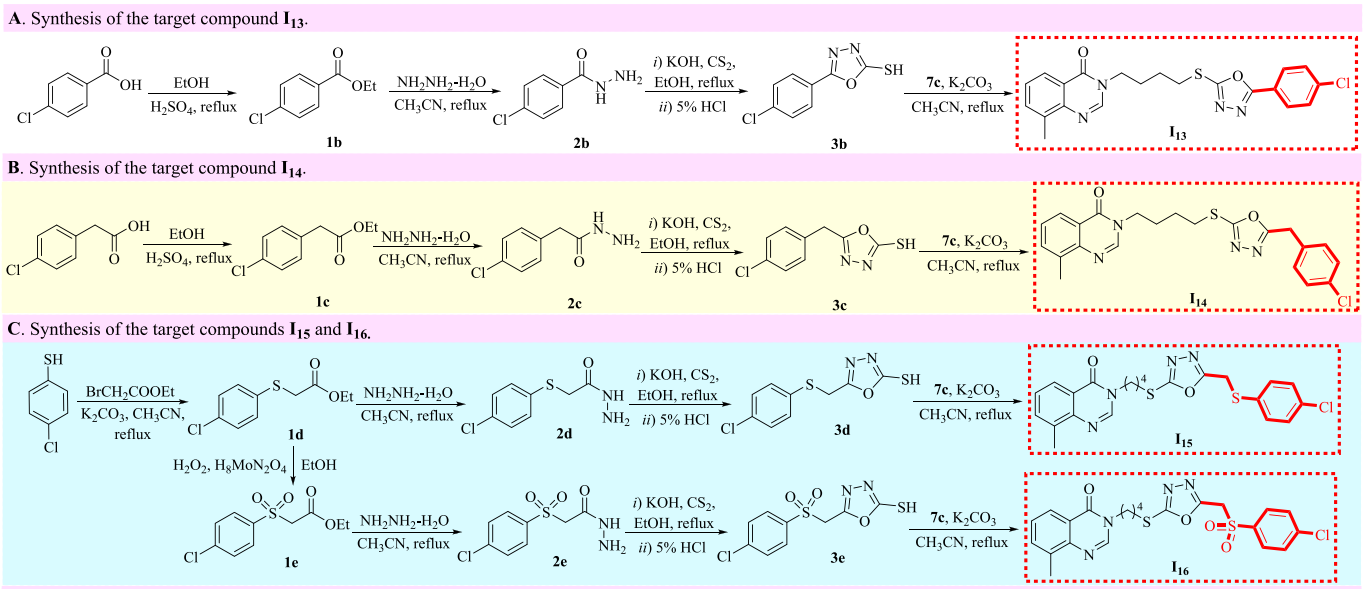

D. Antifungal effects of target compounds I_{13}-I_{16}.

Compound	Antifungal effects at 50 μg/mL (%)				EC_{50} values against *B. cinerea*		
	R. solani	*F. graminearum*	*B. cinerea*	*A. solani*	Regression equation	*r*	EC_{50} (μg/mL)
I_4	50.37 ± 3.02	18.21 ± 0.41	**83.32 ± 3.96**	15.74 ± 0.65	y = 0.59x + 5.02	0.96	**0.92 ± 0.04**
I_{13}	31.44 ± 1.56	29.61 ± 1.75	25.65 ± 0.77	14.64 ± 0.70	/	/	/
I_{14}	57.61 ± 1.71	43.03 ± 2.21	**78.59 ± 0.95**	37.54 ± 1.25	y = 1.26x + 4.29	0.96	**3.66 ± 0.20**
I_{15}	43.15 ± 0.52	36.37 ± 1.15	**69.78 ± 1.22**	17.34 ± 0.55	y = 1.06x + 4.31	0.96	**4.47 ± 0.18**
I_{16}	41.01 ± 1.23	37.52 ± 1.38	30.26 ± 1.13	18.85 ± 0.55	/	/	/

Fig. 5. Synthesis and antifungal effects of target compounds I_{13}–I_{16}.

acetonitrile (25 mL) containing potassium carbonate (7.19 mmol) for 3 h. After filtration, the mentioned-above reactant was desolvated under vacuum, and recrystallized with ethanol to expediently acquire the target molecules I_{13}–I_{16} emerging in Fig. 5.

2.2.5. General procedures for synthesizing target compounds I_{17}–I_{31}

The synthetic methods generating target compounds I_{17}–I_{31} were similar with those that effectively constructed a target compound I_{15}, in which 4-chlorobenzenethiol was replaced by a substituted phenol.

2.3. Antifungal bioassays of title compounds in vitro and in vivo

The tested strains including *Rhizoctonia solani* (*R. solani*), *Fusarium graminearum* (*F. graminearum*), *B. cinerea*, and *Alternaria solani* (*A. solani*) were provided by Jiangsu Key Laboratory of Pesticide Science at Nanjing Agricultural University. Using the agricultural fungicides boscalid, penthiopyral, pyrimethanil and imazalil as four positive controls, the *in vitro* antifungal effects of oxadiazole-containing quinazolin-4(3*H*)-ones against the above four fungi were set three replicates and were evaluated by a mycelia growth rate method that were minutely described in our previously reported work (Chen et al., 2023; Tang et al., 2022; Yang et al., 2022). The anti-*B. cinerea* effects of some bioactive molecules were further tested at five double-declining concentrations for calculating their anti-*B. cinerea* EC_{50} values via a DPS 9.01 software.

Using the fungicides boscalid and penthiopyral exclusively inhibiting *B. cinerea* as two positive controls, the *in vivo* preventative effects of title compound I_{25} against *B. cinerea* were fulfilled on fresh tomato fruits with three replicates (Li et al., 2016; Tai et al., 2023). The tested molecule dissolving in dimethyl sulfoxide (DMSO, 250.00 μL) mixed with the distilled water (50.00 mL) containing azone (1.50 mg), neusilin (1.00 mg) and silicone surfactant (5.00 mg). One day after the resulting mixture was evenly stirred and sprayed on tomato fruits, the newly activated cake of *B. cinerea* was inoculated into the tomato fruits above-mentioned. Thereafter, the tomato fruits inoculated by *B. cinerea* were placed into the environment possessing of 20 °C and 80 % relative humidity. After seven days, the plaque diameter on above tomato fruits was timely measured to calculate the *in vivo* preventative effects of all treatments against *B. cinerea*.

2.4. Studies on morphologies and cell membrane permeabilities

The frozen mycelial dishes treated by I_{25} (25.00 μg/mL) and DMSO were collected according to our reported method, and were observed on a Hitachi SU8010 scanning electron microscopy to smoothly obtain their corresponding SEM images (Chai et al., 2023; Tai et al., 2023). Concurrently, the cell membrane permeabilities of the *B. cinerea* hyphae treated with I_{25} at different concentrations (50.00, 25.00, 12.50, 6.25 and 3.13 μg/mL) were smoothly measured by our previously reported method, in which the *B. cinerea* hyphae treated by DMSO were utilized as a blank control (Chai et al., 2023; Tai et al., 2023).

3. Results and discussion

3.1. Synthesis and in vitro antifungal effects of target compounds I_1–I_6

The impacts of alkyl bridge chains on fungicidal effects were swimmingly investigated by constructing the target compounds I_1–I_6 that contain a different alkyl chain between quinazolin-4(3*H*)-one and 1,3,4-oxadiazole fragments. As shown in Fig. 2**A**, parachlorophenol reacted successively with ethyl bromoacetate ($BrCH_2COOC_2H_5$), hydrazine

hydrate ($NH_2NH_2{\cdot}H_2O$) and carbon disulfide (CS_2) to generate potassium 5-((4-chlorophenoxy)methyl)-1,3,4-oxadiazole-2-thiolate that was acidized with hydrochloric acid to expediently obtain the essential intermediate **3a** named 5-((4-chlorophenoxy)methyl)-1,3,4-oxadiazole-2-thiol. The raw material named 2-amino-3-methylbenzoic acid reacted successively with formamide ($HCONH_2$), formaldehyde (HCHO), sulfoxide chloride ($SOCl_2$) and an intermediate **3a** to successfully generate the target compound $\mathbf{I_1}$ that was structurally confirmed *via* ^{1}H NMR, ^{13}C NMR and HRMS. Concurrently, the obtained 8-methylquinazolin-4(3*H*)-one (**4a**) reacted with a dibromo alkane to synthesize the intermediates **7a**–**7e** that ulteriorly reacted with an intermediate **3a** to construct five target compounds $\mathbf{I_2}$–$\mathbf{I_6}$. Thereafter, the six title compounds $\mathbf{I_1}$–$\mathbf{I_6}$ mentioned-above were measured by a mycelia growth method for their fungicidal effects of against *R. solani*, *F. graminearum*, *B. cinerea* and *A. solani*. The bioassay results in Fig. 2**B** illustrated that the inhibitory effects against four phytopathogenic fungi increased firstly and then decreased with the longness increase of alkyl bridge chains. Strikingly, title compounds $\mathbf{I_2}$ against *R. solani* and $\mathbf{I_4}$ against *B. cinerea* exhibited outstanding fungicidal effects, and their corresponding EC_{50} values reached 11.20 and 0.92 μg/mL, respectively.

3.2. Synthesis and in vitro antifungal effects of target compounds I_7–I_{10}

The salient anti-*B. cinerea* effect of the title compound $\mathbf{I_4}$ inspired the construction of title compounds $\mathbf{I_7}$–$\mathbf{I_{10}}$ that were utilized to explore the effect of quinazolin-4(3*H*)-one fragments on antifungal effects. As shown in Fig. 3**A**, using substituted 2-aminobenzoic acids as raw materials, the target molecules $\mathbf{I_7}$–$\mathbf{I_{10}}$ bearing a different quinazolin-4(3*H*)-one fragment were efficiently synthesized by the methods that were used to construct the title compound $\mathbf{I_4}$. The bioassay results in Fig. 3**B** revealed explicitly the three structure–activity relationships that were expatiated as below. First, the fungicidal effects of target molecules $\mathbf{I_7}$–$\mathbf{I_{10}}$ against *R. solani* and *B. cinerea* overall exceeded 50 % at 50 μg/mL, which were obviously better than those against *F. graminearum* and *A. solani*. Second, the inhibitory effects against *R. solani* at 50 μg/mL could slightly enhance after a quinazolin-4(3*H*)-one fragment ($\mathbf{I_7}$, 44.65 %) was replaced by a 8-methylquinazolin-4(3*H*)-one ($\mathbf{I_4}$, 50.37 %), 6-methylquinazolin-4(3*H*)-one ($\mathbf{I_8}$, 60.37 %), 6-chloroquinazolin-4(3*H*)-one ($\mathbf{I_9}$, 63.78 %) or 6,7-dimethoxyquinazolin-4(3*H*)-one ($\mathbf{I_{10}}$, 61.51 %) fragment. Third, the anti-*B. cinerea* activities of the target molecule $\mathbf{I_4}$ (EC_{50} value = 0.92 μg/mL) declined obviously after replacing the 8-methylquinazolin-4(3*H*)-one fragment in their structure by a quinazolin-4(3*H*)-one ($\mathbf{I_7}$, EC_{50} value = 2.53 μg/mL), 6-methylquinazolin-4(3*H*)-one ($\mathbf{I_8}$, EC_{50} value = 19.52 μg/mL), 6-chloroquinazolin-4(3*H*)-one ($\mathbf{I_9}$, EC_{50} value = 21.76 μg/mL) or 6,7-dimethoxyquinazolin-4(3*H*)-one ($\mathbf{I_{10}}$, EC_{50} value = 54.98 μg/mL) unit. Significantly, Fig. 3**B** also indicated that the 8-methylquinazolin-4(3*H*)-one fragment endowing the outstanding antifungal effects against *B. cinerea* should be unmistakably reserved in the further structural optimization that devoted to developing novel antifungal leads effectively inhibiting *B. cinerea.*

3.3. Synthesis and in vitro antifungal effects of target compounds I_{11} and I_{12}

Aiming to investigate the effects of 1,3,4-oxadiazole fragments on antifungal activities, the target compounds $\mathbf{I_{11}}$ and $\mathbf{I_{12}}$ were logically constructed by replacing the 1,3,4-oxadiazole fragment in the target compound $\mathbf{I_4}$ with a 1,3,4-thiadiazole or 1,2,4-triazole fragment. As shown in Fig. 4**A**, the 2-(4-chlorophenoxy)acetohydrazide (an intermediate **2a**) emerging previously in Fig. 2**A** reacted successively with carbon disulfide and sulfuric acid to generate 5-((4-chlorophenoxy)methyl)-1,3,4-thiadiazole-2-thiol (an intermediate **9**) that subsequently integrated with 3-(4-bromobutyl)-8-methylquinazolin-4(3*H*)-one (an intermediate **7c**) to expediently prepare the 3-(4-((5-((4-chlorophenoxy)methyl)-1,3,4-thiadiazol-2-yl)thio)butyl)-8-methylquinazolin-4(3*H*)-one labeled as a target compound $\mathbf{I_{11}}$. Concurrently, using potassium 2-(2-(4-chlorophenoxy)acetyl)hydrazine-1-carbodithioate (an intermediate **8**) as a beginning reactant, the target compound $\mathbf{I_{12}}$ bearing a 1,2,4-triazole fragment was synthesized by the three successive reactions including the cyclization with hydrazine hydrate, the acidization with hydrochloric acid and the nucleophilic reaction with an intermediate **7c**. The bioassay results in Fig. 4**B** showed that the target compounds $\mathbf{I_4}$, $\mathbf{I_{11}}$ and $\mathbf{I_{12}}$ exhibited the inhibitory selectivity against *B. cinerea* relative to *R. solani*, *F. graminearum* and *A. solani*. Meanwhile, Fig. 4**B** also indicated that the anti-*B. cinerea* EC_{50} value of target molecules slipped significantly after an 1,3,4-oxadiazole fragment ($\mathbf{I_4}$, 0.92 μg/mL) was replaced with a 1,3,4-thiadiazole ($\mathbf{I_{11}}$, 5.31 μg/mL) or 1,2,4-triazole ($\mathbf{I_{12}}$, 69.94 μg/mL) fragment. Strikingly, the antifungal effects against *B. cinerea* followed the order of $\mathbf{I_4} > \mathbf{I_{11}} > \mathbf{I_{12}}$, which evidently reflected the crucial impact of an 1,3,4-oxadiazole fragment on maintaining the anti-*B. cinerea* effects of skeleton molecules.

3.4. Synthesis and in vitro antifungal effects of target compounds I_{13}–I_{16}

The target compounds $\mathbf{I_{13}}$–$\mathbf{I_{16}}$ were immediately constructed to rudimentarily investigate the influence of the substituent at the 5-position of 1,3,4-oxadiazole units on the anti-*B. cinerea* activities of template molecules. As shown in Fig. 5**A**, the esterification of 4-chlorobenzoic acid with ethanol generated ethyl 4-chlorobenzoate **1b** that successively reacted with hydrazine hydrate, carbon disulfide, hydrochloric acid and an intermediate **3a** to construct the target molecule $\mathbf{I_{13}}$ bearing a 4-ClPh fragment. Using 2-(4-chlorophenyl)acetic acid as a raw material, the target molecule $\mathbf{I_{14}}$ bearing a 4-ClBn fragment (Fig. 5**B**) was obtained by the methods synthesizing the target molecule $\mathbf{I_{13}}$. As shown in Fig. 5**C**, the same methods with those synthesizing the target molecule $\mathbf{I_4}$ were again utilized to generate the the target molecule $\mathbf{I_{15}}$ bearing a 4-ClPhSCH_2 fragment with 4-chlorobenzenethiol as an raw material. After the ethyl 2-((4-chlorophenyl)thio)acetate **1d** emerging in Fig. 5**C** was oxidated, the synthesized ethyl 2-((4-chlorophenyl)sulfonyl)acetate **1e** reacted successively with hydrazine hydrate, carbon disulfide, hydrochloric acid and an intermediate **3a** to construct the target molecule $\mathbf{I_{16}}$ bearing a 4-ClPhSO_2CH_2 fragment. The bioassay results in Fig. 5**D** showed that the target compounds $\mathbf{I_4}$ and $\mathbf{I_{13}}$–$\mathbf{I_{16}}$ exhibited overall the excellent selectivity against *B. cinerea* relative to *R. solani*, *F. graminearum* and *A. solani* at 50 μg/mL. Meanwhile, Fig. 5**D** also indicated that the anti-*B. cinerea* effects followed approximately the order of $\mathbf{I_4}$ (EC_{50} value = 0.92 μg/mL) > $\mathbf{I_{14}}$ (EC_{50} value = 3.66 μg/mL) > $\mathbf{I_{15}}$ (EC_{50} value = 4.47 μg/mL) > $\mathbf{I_{16}}$ (EC_{50} value = over 50.00 μg/mL) > $\mathbf{I_{13}}$ (EC_{50} value = over 50.00 μg/mL).

3.5. Synthesis and in vitro antifungal effects of target compounds I_{17}–I_{31}

The bioassays results in Fig. 5**D** evidently reflected that the anti-*B. cinerea* performances of target molecules correlated closely with the phenoxymethyl fragment at the 5-position of 1,3,4-oxadiazole scaffolds. Aiming to meticulously explore the phenoxymethyl fragment at the 5-position of 1,3,4-oxadiazole scaffolds toward anti-*B. cinerea* activities, the target compounds $\mathbf{I_{17}}$–$\mathbf{I_{31}}$ (Fig. 6**A**) were purposively constructed by the synthetic methods that were utilized to smoothly prepare a target compounds $\mathbf{I_4}$. Subsequently, the inhibitory effects against *R. solani*, *F. graminearum*, *A. solani* and *B. cinerea* were evaluated and summerized in Fig. 6**B** that clearly presented the below three structure–activity relationships. Firstly, the inhibitory effects of all phenoxymethyl-containing molecules against *B. cinerea* exceed 74 % at 50.00 μg/mL, which were obviously better than those against *R. solani*, *F. graminearum* and *A. solani*. Secondly, the anti-*B. cinerea* effects of target molecules did not enhance effectively after superseding the hydrogen atom ($\mathbf{I_{17}}$, R = Ph, EC_{50} value = 2.16 μg/mL) at the *meta*-position of benzene rings by a chlorine atom ($\mathbf{I_{19}}$, Ar = 3-ClPh, EC_{50} value = 2.25 μg/mL; $\mathbf{I_{27}}$, Ar = 3,5-di-ClPh, EC_{50} value = 2.10 μg/mL), a methoxy group ($\mathbf{I_{23}}$, R = 3-MeOPh, EC_{50} value = 4.95 μg/mL) or a methyl fragment ($\mathbf{I_{28}}$, R = 3,5-di-MePh, EC_{50} value = 2.52 μg/mL). Thirdly, introducing a chlorine atom ($\mathbf{I_4}$, Ar

A. Synthesis of target compounds I_{17}-I_{31}.

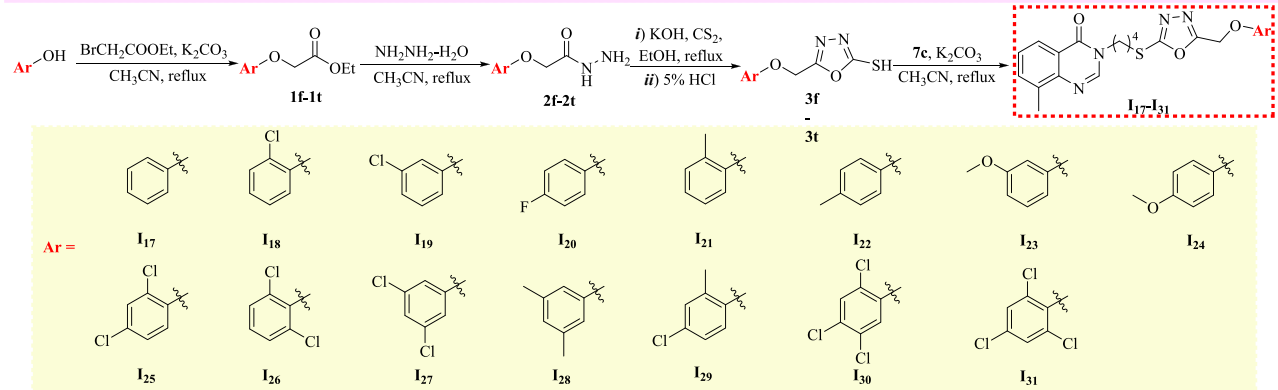

B. Antifungal effects of target compounds I_{17}-I_{31}.

Compound	Antifungal effects at 50 μg/mL (%)				EC_{50} values against *B. cinerea*		
	R. solani	*F. graminearum*	*B. cinerea*	*A. solani*	Regression equation	*r*	EC_{50} (μg/mL)
I_4	50.37 ± 3.02	18.21 ± 0.41	**83.32 ± 3.96**	15.74 ± 0.65	y = 0.59x + 5.02	0.96	**0.92 ± 0.04**
I_{17}	**63.63 ± 1.37**	57.15 ± 2.02	**85.46 ± 0.86**	23.96 ± 1.10	y = 1.11x + 4.63	0.99	2.16 ± 0.23
I_{18}	**71.18 ± 1.28**	42.71 ± 2.16	**81.21 ± 0.77**	2.33 ± 0.22	y = 0.73x + 5.07	0.97	**0.80 ± 0.11**
I_{19}	38.31 ± 1.04	32.14 ± 1.52	**93.63 ± 0.81**	2.71 ± 0.15	y = 0.84x + 4.70	0.96	2.25 ± 0.15
I_{20}	51.83 ± 0.81	48.00 ± 0.55	**87.37 ± 0.81**	12.73 ± 0.65	y = 1.14x + 4.64	0.99	**2.05 ± 0.21**
I_{21}	49.69 ± 1.19	22.71 ± 0.60	**83.47 ± 1.76**	17.02 ± 0.18	y = 0.76x + 4.99	0.96	**1.02 ± 0.08**
I_{22}	44.48 ± 2.04	44.09 ± 0.87	**79.40 ± 1.49**	8.22 ± 0.65	y = 0.64x + 4.91	0.91	**1.36 ± 0.11**
I_{23}	**74.82 ± 1.14**	36.74 ± 1.70	**87.37 ± 1.49**	2.21 ± 0.65	y = 1.23x + 4.14	0.99	4.95 ± 0.39
I_{24}	52.30 ± 4.60	47.54 ± 1.75	78.50 ± 1.04	5.71 ± 0.60	y = 0.77x + 4.72	0.96	2.30 ± 0.36
I_{25}	49.08 ± 2.13	50.23 ± 2.09	**85.20 ± 1.22**	2.13 ± 0.92	y = 0.63x + 5.07	0.99	**0.76 ± 0.05**
I_{26}	27.41 ± 1.23	30.30 ± 0.78	**84.44 ± 0.77**	4.46 ± 0.35	y = 0.62x + 4.98	0.95	**1.09 ± 0.03**
I_{27}	50.17 ± 0.62	39.49 ± 1.33	**83.75 ± 0.72**	17.24 ± 0.65	y = 0.92x + 4.70	0.97	**2.10 ± 0.14**
I_{28}	47.80 ±1.28	23.86 ± 1.24	**89.24 ± 1.08**	5.12 ± 0.32	y = 1.13x + 4.55	0.99	2.52 ± 0.11
I_{29}	50.40 ± 0.81	40.64 ± 1.98	**80.98 ± 1.72**	5.21 ± 0.25	y = 0.70x + 4.94	0.99	**1.22 ± 0.08**
I_{30}	36.04 ± 0.52	53.15 ± 1.20	74.14 ± 1.17	3.81 ± 1.30	y = 0.64x + 4.68	0.91	3.20 ± 0.19
I_{31}	29.30 ± 1.56	27.31 ± 2.21	**88.56 ± 1.22**	3.71 ± 0.10	y = 0.84x + 4.73	0.98	**2.10 ± 0.16**
DMSO	1.26 ± 0.21	0.34 ± 0.00	1.57 ± 0.41	2.17 ± 0.73	/	/	/
Boscalid	85.06 ± 1.00	23.91 ± 0.18	98.65 ± 1.49	60.15 ± 1.20	y = 0.70x + 5.04	0.98	0.86 ± 0.06
Penthiopyral	97.65 ± 2.17	56.84 ± 2.24	95.48 ± 2.12	47.76 ± 0.96	y = 0.79x + 4.99	0.97	1.03 ± 0.11
Pyrimethanil	32.36 ± 1.57	34.12 ± 1.22	79.39 ± 0.61	29.14 ± 0.82	y = 2.80x + 1.63	0.98	15.91 ± 0.16
Imazalil	98.76 ± 1.73	68.66 ± 1.73	99.75 ± 3.36	94.78 ± 1.66	y = 1.37x + 4.54	0.99	2.15 ± 0.33

Fig. 6. Synthesis and antifungal effects of target compounds I_{17}–I_{31}.

= 4-ClPh, EC_{50} value = 0.92 μg/mL; I_{18}, Ar = 2-ClPh, EC_{50} value = 0.80 μg/mL) or a methyl fragment (I_{21}, Ar = 2-MePh, EC_{50} value = 1.02 μg/mL; I_{22}, Ar = 4-MePh, EC_{50} value = 1.36 μg/mL) into the ortho- or *para*-positions could praiseworthily improve the anti-*B. cinerea* effects of skeleton molecules. The above structure–activity relationships reasonably inspired the construction of target compounds I_{25}, I_{26} and I_{29}–I_{31}. Among five constructed molecules, the target compound I_{25} (Ar = 2,4-di-ClPh) exhibited strikingly the best antifungal effect against *B. cinerea* with the EC_{50} value of 0.76 μg/mL (Fig. 7) that was obviously superior to those of boscalid (0,86 μg/mL), penthiopyral (1.03 μg/mL), pyrimethanil (15.91 μg/mL) and imazalil (2.15 μg/mL).

3.6. *Effects of a bioactive molecule I_{25} on the hyphal morphology and cell membrane permeability of B. cinerea*

The impacts of a target molecule I_{25} on the hyphal morphology of *B. cinerea* were investigated by a SEM that utilized the *B. cinerea* hyphae treated by DMSO as a blank control. The collected SEM images of the *B. cinerea* hyphae treated by DMSO and I_{25} were respectively presented in Fig. 8**A–C** and Fig. 8**D–F**. Featuring plump and smooth structures, the *B. cinerea* hyphae in Fig. 8**A–C** not entangled with each other and proliferated all around the surface of the PDA medium containing DMSO. After treated by a target molecule I_{25} at 25 μg/mL, the hyphal morphology of *B. cinerea* (Fig. 8**D–F**) generated two distinctive changes. Firstly, the hyphal surface of *B. cinerea* appeared conspicuous wrinkles and concavo-convex phenomena, as shown in Fig. 8**E–F**, which was the

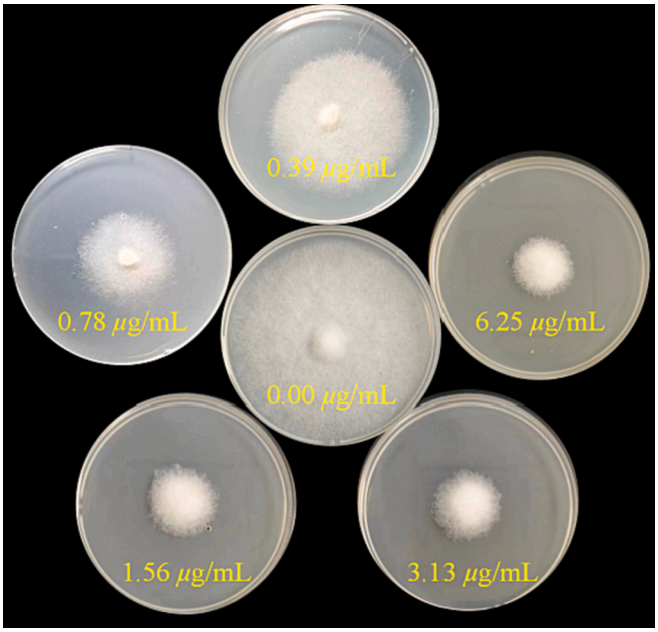

Fig. 7. Antifungal effects of a target compound $\mathbf{I_{25}}$ against *B. cinerea.*

most prominent alteration caused by a target molecule $\mathbf{I_{25}}$. Secondly, the mycelia in Fig. 8**E–F** formed the abnormal aggregation by the reciprocal entanglements that were also obviously different with the hyphal morphologies in Fig. 8**B–C**. Inspired by the above tremendous alteration on hyphal surfaces, we ulteriorly determined the influence of a target molecule $\mathbf{I_{25}}$ on the cell membrane permeability of *B. cinerea* hyphae. As revealed vividly in Fig. 9, the cell membrane permeability of *B. cinerea* hyphae increased gradually with the consistent increase of a target molecule $\mathbf{I_{25}}$, which confirmed again the pivotal influence of constructed quinazolin-4(3*H*)-one bionic-alkaloids on the cell membrane of *B. cinerea* hyphae.

3.7. *In vivo preventative effect of a molecule* $\mathbf{I_{25}}$ *against B. cinerea*

The systematical optimizations revolving around oxadiazole-containing quinazolin-4(3*H*)-one structures generated the promising anti-*B. cinerea* candidate $\mathbf{I_{25}}$ owning the fantastic EC_{50} value of 0.76 μg/mL that was superior to those of boscalid (0.86 μg/mL), penthiopyral (1.03 μg/mL), pyrimethanil (15.91 μg/mL) and imazalil (2.15 μg/mL). Encouraged by the *in vitro* anti-*B. cinerea* performance mentioned-above, the *in vivo* preventative effect of a quinazolin-4(3*H*)-one molecule $\mathbf{I_{25}}$ against *B. cinerea* was further evaluated at 200 μg/mL on fresh tomato fruits. Concurrently, boscalid and penthiopyrad, two commercialized fungicide effectively inhibiting *B. cinerea*, were utilized as the positive controls to examine the application values of a quinazolin-4(3*H*)-one molecule $\mathbf{I_{25}}$ as potential agricultural fungicides. As vividly presented in Fig. 10, the *in vivo* preventative efficacy of an active molecule $\mathbf{I_{25}}$ against *B. cinerea* strikingly reached 69.3 % at 200 μg/mL, which was megascopically better than that of boscalid (60.6 %) under same conditions. The above *in vivo* bioassay results reflected convincingly the possibility of oxadiazole-containing quinazolin-4(3*H*)-one bionic-alkaloids as the promising fungicide alternatives inhibiting *B. cinerea*.

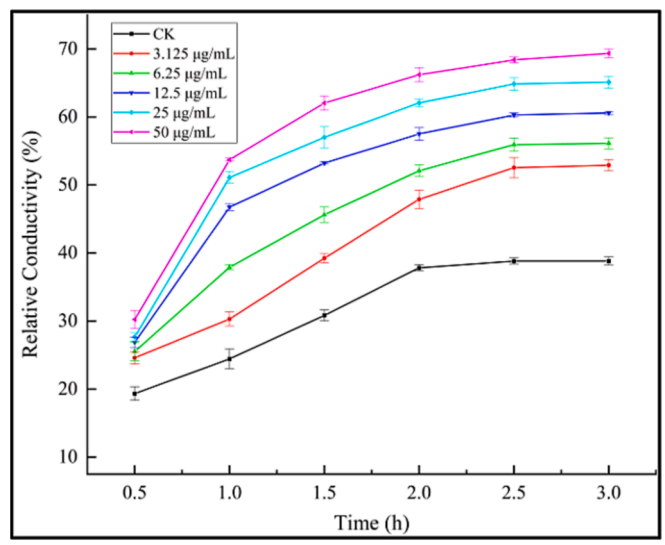

Fig. 9. Effects of a bioactive molecule $\mathbf{I_{25}}$ on the cell membrane permeability of *B. cinerea.*

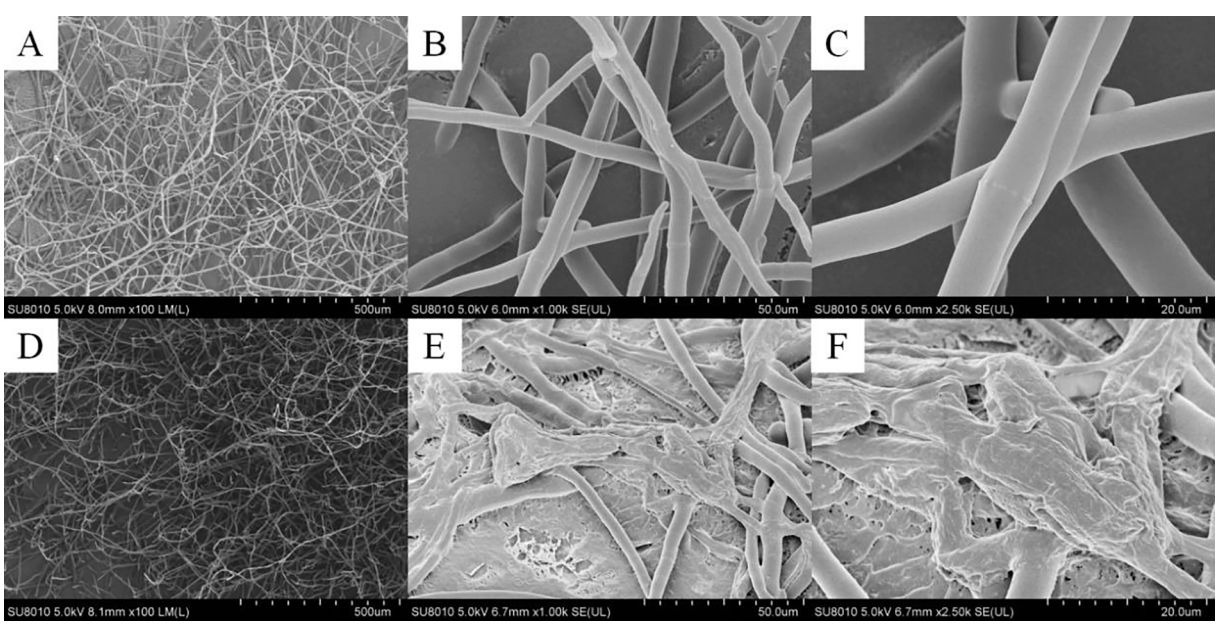

Fig. 8. SEM images of the *B. cinerea* hyphae treated by DMSO (**A–C**) and $\mathbf{I_{25}}$ (**D–F**).

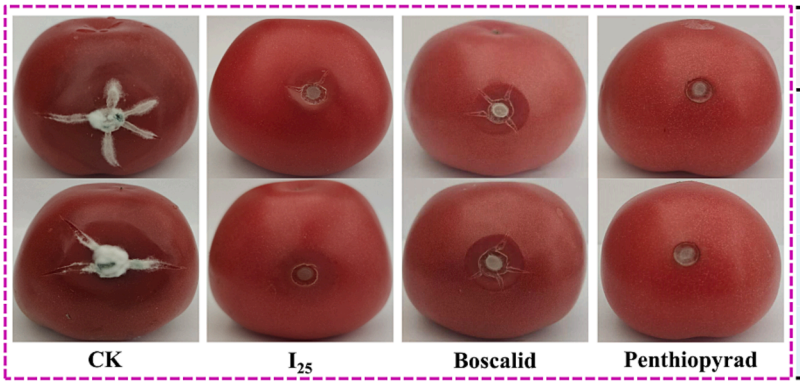

Treatment	Preventative efficacy (%)
$\mathbf{I_{25}}$	69.3 ± 2.1
Boscalid	60.6 ± 3.6
Penthiopyrad	80.3 ± 1.8
CK	—

Fig. 10. *In vivo* preventative effects of a molecule $\mathbf{I_{25}}$ against *B. cinerea* at 200 μg/mL.

4. Conclusions

Aiming to develop novel antifungal leads featuring a inimitable action mechanism against *B. cinerea*, thirty-one oxadiazole-containing quinazolin-4(3*H*)-one bionic-alkaloids were rationally designed, synthesized and structurally verified by corresponding ^{1}H NMR, ^{13}C NMR and HRMS analyses. The systematical optimization on oxadiazole-containing quinazolin-4(3*H*)-one structures generated the promising anti-*B. cinerea* candidate $\mathbf{I_{25}}$ owning the *in vitro* EC_{50} value of 0.76 μg/mL that was fantastically superior to those of boscalid, penthiopyral, pyrimethanil and imazalil (0.86, 1.03, 15.91 and 2.15 μg/mL, respectively). The further studies on morphologies and cell membrane permeabilities indicated that the fungicidal molecule $\mathbf{I_{25}}$ could induce the conspicuous wrinkle on hyphal surfaces and increase the membrane permeability of *B. cinerea* cells. Whereafter, the *in vivo* preventative efficacy of an active molecule $\mathbf{I_{25}}$ against *B. cinerea* was noticeably evaluated as 69.3 % at 200 μg/mL, which was megascopically better than that of boscalid (60.6 %) under same conditions. Further studies on the anti-*B. cinerea* mechanism and structural modification of oxadiazole-containing quinazolin-4(3*H*)-one bionic-alkaloids are currently underway.

Declaration of Competing Interest

The authors declare that they have no known competing financial interests or personal relationships that could have appeared to influence the work reported in this paper.

Acknowledgments

Authors gratefully acknowledge the grants from the National Natural Science Foundation of China (Nos. 32202334 and 22301109), the Natural Science Foundation of Jiangsu University (No. 22KJB210009), the Research Funds for Talent Introduction of Jiangsu Ocean University (No. KQ21031), and the Postgraduate Research & Practice Innovation Program of Jiangsu Ocean University (No. KYCX202340).

Appendix A. Supplementary data

The physical and spectroscopic data of novel constructed compounds $\mathbf{I_7}$–$\mathbf{I_{31}}$ were provided in the Supporting Information. All the copies of the above ^{1}H NMR, ^{13}C NMR and HRMS spectrogram were neatened in the Supporting Information.

Supplementary data to this article can be found online at https://doi.org/10.1016/j.arabjc.2023.105455.

References

Almalki, A.S.A., Nazreen, S., Elbehairi, S.E.I., Asad, M., Shati, A.A., Alfaifi, M.Y., Alhadhrami, A., Elhenawy, A.A., Alorabi, A.Q., Asiri, A.M., Alam, M.M., 2022. Design, synthesis, anticancer activity and molecular docking studies of new benzimidazole derivatives bearing 1,3,4-oxadiazole moieties as potential thymidylate synthase inhibitors. New. J. Chem. 46, 14967–14978. https://doi.org/10.1039/D2NJ01980A.

Bardas, G.A., Veloukas, T., Koutita, O., Karaoglanidis, G.S., 2010. Multiple resistance of *Botrytis cinerea* from kiwifruit to SDHIs, QoIs and fungicides of other chemical groups. Pest Manag. Sci. 66, 967–973. https://doi.org/10.1002/ps.1968.

Chai, J.Q., Mei, Y.D., Tai, L., Wang, X.B., Chen, M., Kong, X.Y., Lu, A.M., Li, G.H., Yang, C.L., 2023. Potential succinate dehydrogenase inhibitors bearing a novel pyrazole-4-sulfonohydrazide scaffold: Molecular design, antifungal evaluation, and action mechanism. J. Agric. Food Chem. 71, 9266–9279. https://doi.org/10.1021/acs.jafc.3c00126.

Chen, H., Li, Z., Han, Y., 2000. Synthesis and fungicidal activity against Rhizoctonia solani of 2-alkyl (alkylthio)-5-pyrazolyl-1,3,4-oxadiazoles (thiadiazoles). J. Agric. Food Chem. 48, 5312–5315. https://doi.org/10.1021/jf991065s.

Chen, S., Zhang, M., Feng, S., Gong, C., Zhou, Y., Xing, L., He, B., Wu, Y., Xue, W., 2023. Design, synthesis and biological activity of chalcone derivatives containing pyridazine. Arabian J. Chem. 16, 104852 https://doi.org/10.1016/j.arabjc.2023.104852.

Dean, R., Vankan, J.A.L., Pretorius, Z.A., Hammond-Kosack, K.E., Pietro, A.D., Spanu, P. D., Rudd, J.J., Dickman, M., Kahmann, R., Ellis, J., Foster, G.D., 2012. The top 10 fungal pathogens in molecular plant pathology. Mol. Plant Pathol. 13, 414–430. https://doi.org/10.1111/j.1364-3703.2011.00783.x.

Dong, J., Gao, W., Li, K., Hong, Z., Tang, L., Han, L., Wang, Z., Fan, Z., 2022. Design, synthesis, and biological evaluation of novel psoralen-based 1,3,4-oxadiazoles as potent fungicide candidates targeting pyruvate kinase. J. Agric. Food Chem. 70, 3435–3446. https://doi.org/10.1021/acs.jafc.1c07911.

Du, H., Fan, Z., Yang, L., Bao, X., 2018. Synthesis and antimicrobial activities of novel 1,2,4-triazole-acyl-hydrazone derivatives containing the quinazolin-4-one moiety. Chin. J. Org. Chem. 38, 531–538. https://doi.org/10.6023/cjoc201708051.

Gao, M., Yu, L., Li, P., Song, X., Chen, Z., He, M., Song, B., 2017. Label-free quantitative proteomic analysis of inhibition of *Xanthomonas axonopodis pv. citri* by the novel bactericide Fubianezuofeng. Pestic. Biochem. Physiol. 138, 37–42. https://doi.org/10.1016/j.pestbp.2017.02.004.

Hao, Y., Guo, J., Wang, Z., Liu, Y., Li, Y., Ma, D., Wang, Q., 2020. Discovery of tryptanthrins as novel antiviral and anti-phytopathogenic-fungus agents. J. Agric. Food Chem. 68, 5586–5595. https://doi.org/10.1021/acs.jafc.0c02101.

Harper, L.A., Paton, S., Hall, B., Mckay, S., Oliver, R.P., Lopea-Ruiz, F.J., 2022. Fungicide resistance characterized across seven modes of action in *Botrytis cinerea* isolated from Australian vineyards. Pest Manag. Sci. 78, 1326–1340. https://doi.org/10.1002/ps.6749.

Hou, S., Shi, H., Zhang, H., Wu, Z., Hu, D., 2023. Synthesis, antifungal evaluation, 3D-QSAR, and preliminarily mechanism study of novel chiral mandelic acid derivatives. J. Agric. Food Chem. 71, 7631–7641. https://doi.org/10.1021/acs.jafc.2c09006.

Jian, W., He, D., Xi, P., Li, X., 2015. Synthesis and biological evaluation of novel fluorine-containing stilbene derivatives as fungicidal agents against phytopathogenic fungi. J. Agric. Food Chem. 63, 9963–9969. https://doi.org/10.1021/acs.jafc.5b04367.

Khanum, S.A., Shashikanth, S., Sathyanarayana, S.G., Lokesh, S., Deepak, S.A., 2009. Synthesis and antifungal activity of 2-azetidinonyl-5-(2-benzoylphenoxy)methyl-1,3,4-oxadiazoles against seed-borne pathogens of Eleusine coracana (L.) Gaertn. Pest Manag. Sci. 65, 776–780. https://doi.org/10.1002/ps.1752.

Li, S., Li, D., Xiao, T., Zhang, S., Song, Z., Ma, H., 2016. Design, synthesis, fungicidal activity, and unexpected docking model of the first chiral boscalid analogues containing oxazolines. J. Agric. Food Chem. 64, 8927–8934. https://doi.org/10.1021/acs.jafc.6b03464.

Liu, S., Che, Z., Chen, G., 2016. Multiple-fungicide resistance to carbendazim, diethofencarb, procymidone, and pyrimethanil in field isolates of *Botrytis cinerea* from tomato in Henan Province, China. Crop Prot. 84, 56–61. https://doi.org/10.1016/j.cropro.2016.02.012.

Long, Z.Q., Yang, L.L., Zhang, J.R., Liu, S.T., Xie, J., Wang, P.Y., Zhu, J.J., Shao, W.B., Liu, L.W., Yang, S., 2021. Fabrication of versatile pyrazole hydrazide derivatives bearing a 1,3,4-oxadiazole core as multipurpose agricultural chemicals against plant fungal, oomycete, and bacterial diseases. J. Agric. Food Chem. 69, 8380–8393. https://doi.org/10.1021/acs.jafc.1c02460.

Lv, X.L., Yang, L., Fan, Z., Bao, X., 2018. Synthesis and antimicrobial activities of novel quinazolin-4(3H)-one derivatives containing a 1,2,4-triazolo[3,4-b][1,3,4]thiadiazole moiety. J. Saudi Chem. Soc. 22, 101–109. https://doi.org/10.1016/j.jscs.2017.07.008.

Ma, L., Xiao, Y., Li, C., Xie, Z.L., Li, D.D., Wang, Y.T., Ma, H.T., Zhu, H.L., Wang, M.H., Ye, Y.H., 2013. Synthesis and antioxidant activity of novel Mannich base of 1,3,4-oxadiazole derivatives possessing 1,4-benzodioxan. Bioorg. Med. Chem. 21, 6763–6770. https://doi.org/10.1016/j.bmc.2013.08.002.

Peng, F., Liu, T., Wang, Q., Liu, F., Cao, X., Yang, J., Liu, L., Xie, C., Xue, W., 2021. Antibacterial and antiviral activities of 1,3,4-oxadiazole thioether *4*H-chromen-4-one derivatives. J. Agric. Food Chem. 69, 11085–11094. https://doi.org/10.1021/acs.jafc.1c03755.

Petrasch, S., Knapp, S.J., Vankan, J.A.L., Blanco-Ulate, B., 2019. Grey mould of strawberry, a devastating disease caused by the ubiquitous necrotrophic fungal pathogen *Botrytis cinerea*. Mol. Plant Pathol. 20, 877–892. https://doi.org/10.1111/mpp.12794.

Rapolu, S., Alla, M., Bommena, V.R., Murthy, R., Jain, N., Bommareddy, V.R., Bommineni, M.R., 2013. Synthesis and biological screening of 5-(alkyl(1H-indol-3-yl))-2- (substituted)-1,3,4-oxadiazoles as antiproliferative and anti-inflammatory agents. Eur. J. Med. Chem. 66, 91–100. https://doi.org/10.1016/j.ejmech.2013.05.024.

Rasool, N., Razzaq, Z., Khan, S.G., Javaid, S., Akhtar, N., Mahmood, S., Christensen, J.B., Altaf, A.A., Anjum, S.M.M., Alqahtani, F., Alasmari, A.F., Imran, I., 2023. A facile synthesis of 1,3,4-oxadiazole-based carbamothioate molecules: Antiseizure potential, EEG evaluation and *in-silico* docking studies. Arabian J. Chem. 16, 104610 https://doi.org/10.1016/j.arabjc.2023.104610.

Shao, W., Zhao, Y., Ma, Z., 2021. Advances in understanding fungicide resistance in *Botrytis cinerea* in China. Phytopathology 111, 455–463. https://doi.org/10.1094/PHYTO-07-20-0313-IA.

Tai, L., Sun, S.X., Yue, K., Chai, J.Q., Hou, S.T., Dai, G.Y., Yang, C.L., Chen, M., 2023. Novel fungicidal phenylethanol derivatives linking a trifluoromethyl pyrazole pharmacophore: Design, synthesis, crystal structure, and biology evaluation. New J. Chem. 47, 12850–12860. https://doi.org/10.1039/D3NJ02234J.

Tang, X., Zhan, W., Chen, S., Zhou, R., Hu, D., Sun, N., Fei, Q., Wu, W., Xue, W., 2022. Synthesis, bioactivity and preliminary mechanism of action of novel trifluoromethyl pyrimidine derivatives. Arabian J. Chem. 15, 104110 https://doi.org/10.1016/j.arabjc.2022.104110.

Tantray, M.A., Khan, I., Hamid, H., Alam, M.S., Dhulap, A., Kalam, A., 2018. Synthesis of benzimidazole-linked-1,3,4-oxadiazole carboxamides as GSK-3b inhibitors with in vivo antidepressant activity. Bioorg. Chem. 77, 393–401. https://doi.org/10.1016/j.bioorg.2018.01.040.

Tao, Q.Q., Liu, L.W., Wang, P.Y., Long, Q.S., Zhao, Y.L., Jin, L.H., Xu, W.M., Chen, Y., Li, Z., Yang, S., 2019. Synthesis and *in vitro* and *in vivo* biological activity evaluation and quantitative proteome profiling of oxadiazoles bearing flexible heterocyclic patterns. J. Agric. Food Chem. 67, 7626–7639. https://doi.org/10.1021/acs.jafc.9b02734.

Wang, X., Li, P., Li, Z., Yin, J., He, M., Xue, W., Chen, Z., Song, B., 2013. Synthesis and bioactivity evaluation of novel arylimines containing a 3-aminoethyl-2-[(p-trifluoromethoxy)anilino]-4(3H)-quinazolinone moiety. J. Agric. Food Chem. 61, 9575–9582. https://doi.org/10.1021/jf403193q.

Wang, X., Wang, M., Yan, J., Chen, M., Wang, A., Mei, Y., Si, W., Yang, C., 2018. Design, synthesis and 3D-QSAR of new quinazolin-4(3H)-one derivatives containing a hydrazide moiety as potential fungicides. ChemistrySelect 3, 10663–10669. https://doi.org/10.1002/slct.201801575.

Wang, X., Hu, H., Zhao, X., Chen, M., Zhang, T., Geng, C., Mei, Y., Lu, A., Yang, C., 2019. Novel quinazolin-4(3H)-one derivatives containing an 1,3,4-oxadiazole thioether moiety as potential bactericides and fungicides: Design, synthesis, characterization and 3D-QSAR analysis. J. Saudi Chem. Soc. 23, 1144–1156. https://doi.org/10.1016/j.jscs.2019.07.006.

Wang, X., Chai, J., Kong, X., Jin, F., Chen, M., Yang, C., Xue, W., 2021. Expedient discovery for novel antifungal leads: 1,3,4-Oxadiazole derivatives bearing a quinazolin-4(3H)-one fragment. Bioorg. Med. Chem. 45, 116330 https://doi.org/10.1016/j.bmc.2021.116330.

Wang, X., Chai, J., Gu, Y., Zhang, D., Meng, F., Si, X., Yang, C., Xue, W., 2022. Expedient discovery for novel antifungal leads inhibiting Fusarium graminearum: 3-(Phenylamino)quinazolin-4(3H)-ones deriving from systematic optimizations on a tryptanthrin structure. J. Agric. Food Chem. 70, 13165–13175. https://doi.org/10.1021/acs.jafc.2c04933.

Wang, X.Q., Liu, J., Zhang, N., Yang, H., 2020. Adsorption, mobility, biotic and abiotic metabolism and degradation of pesticide exianliumi in three types of farmland. Chemosphere 254, 126741. https://doi.org/10.1016/j.chemosphere.2020.126741.

Wang, F., Yang, B.X., Zhang, T.H., Tao, Q.Q., Zhou, X., Wang, P.Y., Yang, S., 2023. Novel 1,3,4-oxadiazole thioether and sulfone derivatives bearing a flexible *N*-heterocyclic moiety: Synthesis, characterization, and anti-microorganism activity. Arabian J. Chem. 16, 104479 https://doi.org/10.1016/j.arabjc.2022.104479.

Williamson, B., Tudzynski, B., Tudzynski, P., Vankan, J.A.L., 2007. *Botrytis cinerea*: the cause of grey mould disease. Mol. Plant Pathol. 8, 561–580. https://doi.org/10.1111/j.1364-3703.2007.00417.x.

Xiong, F., Liu, M., Zhuo, F., Yin, H., Deng, K., Feng, S., Liu, Y., Luo, X., Feng, L., Zhang, S., Li, Z., Ren, M., 2019. Host-induced gene silencing of *BcTOR* in *Botrytis cinerea* enhances plant resistance to grey mould. Mol. Plant Pathol. 20, 1722–1739. https://doi.org/10.1111/mpp.12873.

Xu, W., Yang, S., Bhadury, P., He, J., He, M., Gao, L., Hu, D., Song, B., 2011. Synthesis and bioactivity of novel sulfone derivatives containing 2,4-dichlorophenyl substituted 1,3,4-oxadiazole/thiadiazole moiety as chitinase inhibitors. Pestic. Biochem. Physiol. 101, 6–15. https://doi.org/10.1016/j.pestbp.2011.05.006.

Yang, Z., Sun, Y., Liu, Q., Li, A., Wang, W., Gu, W., 2021. Design, synthesis, and antifungal activity of novel thiophene/furan-1,3,4-oxadiazole carboxamides as potent succinate dehydrogenase inhibitors. J. Agric. Food Chem. 69, 13373–13385. https://doi.org/10.1021/acs.jafc.1c03857.

Yang, J., Xie, D., Zhang, C., Zhao, C., Wu, Z., Xue, W., 2022. Synthesis, antifungal activity and *in vitro* mechanism of novel 1-substituted-5-trifluoromethyl-1*H*-pyrazole-4-carboxamide derivatives. Arabian J. Chem. 15, 103987 https://doi.org/10.1016/j.arabjc.2022.103987.

Yang, G.Z., Zhan, J., Peng, J.W., Zhang, Z.J., Zhao, W.B., Wang, R.X., Ma, K.Y., Li, J.C., Liu, Y.Q., Zhao, Z.M., Shang, X.F., 2020. Discovery of luotonin A analogues as potent fungicides and insecticides: Design, synthesis and biological evaluation inspired by natural alkaloid. Eur. J. Med. Chem. 194, 112253 https://doi.org/10.1016/j.ejmech.2020.112253.

Zhang, Z.J., Jiang, Z.Y., Zhu, Q., Zhong, G.H., 2018. Discovery of β-carboline oxadiazole derivatives as fungicidal agents against rice sheath blight. J. Agric. Food Chem. 66, 9598–9607. https://doi.org/10.1021/acs.jafc.8b02124.

Zhang, J., Liu, J., Ma, Y., Ren, D., Cheng, P., Zhao, J., Zhang, F., Yao, Y., 2016. One-pot synthesis and antifungal activity against plant pathogens of quinazolinone derivatives containing an amide moiety. Bioorg. Med. Chem. Lett. 26, 2273–2277. https://doi.org/10.1016/j.bmcl.2016.03.052.

Zhu, J.J., Wang, P.Y., Long, Z.Q., Xiang, S.Z., Zhang, J.R., Li, Z.X., Wu, Y.Y., Shao, W.B., Zhou, X., Liu, L.W., Yang, S., 2022. Design, synthesis, and biological profiles of novel 1,3,4-oxadiazole-2-carbohydrazides with molecular diversity. J. Agric. Food Chem. 70, 2825–2838. https://doi.org/10.1021/acs.jafc.1c07190.

Zou, X.J., Lai, L.H., Jin, G.Y., Zhang, Z.X., 2002. Synthesis, fungicidal activity, and 3D-QSAR of pyridazinone-substituted 1,3,4-oxadiazoles and 1,3,4-thiadiazoles. J. Agric. Food Chem. 50, 3757–3760. https://doi.org/10.1021/jf0201677.